AIAA 80-0270R

Upper Surface Blown Airfoils in Incompressible and Transonic Flows

N. D. Malmuth,* W. D. Murphy,† and V. Shankar†
Rockwell International Science Center, Thousand Oaks, Calif.

J. D. Cole‡
University of California, Los Angeles, Calif.
and
E. Cumberbatch§
Purdue University, West Lafayette, Ind.

Asymptotic and computational methods have been utilized to study the incompressible and transonic flow over upper surface blown airfoils. In the models discussed, the problem has been decomposed into the treatment of the fine structure of the jet and the analysis of the flow outside of it. Asymptotic expansions of limit process type have been used to treat the jet in a thin-layer approximation using suitable strained variables. Although vorticity must be accounted for in matching with the external flow, its effect on the Spence boundary conditions derived under irrotational assumptions is nil in regions away from the trailing edge and jet exit. A similar conclusion applies for compressibility. The condition of flow pressure and direction compatibility replacing the Kutta condition for the unblown configuration indicates that the dividing streamline leaves the higher total head upper surface of the airfoil tangent to the trailing edge. Computational results for an upper surface blowing airfoil indicate significant enhancements in lift with blowing. Comparisons with experiments indicate that viscous wall jet effects, wave interaction phenomena with the mixing zones near the jet exit, and trailing-edge layers must be incorporated into the model for improved simulation of the flow physics.

I. Introduction

UPPER surface blowing (USB) has been proposed as a means of increasing usable lift and thereby enhancing V/STOL capability at low speeds in landing configurations. At transonic Mach numbers, it has the further application of achieving low turn radii in dogfight scenarios. The attendant high accelerations are accomplished through elimination of separation by suppression of adverse pressure gradients in the viscous boundary layer, and also movement of shocks downstream of the trailing edge, thereby discouraging shock induced separation and buffet at high maneuver incidences. Further applications of laminar flow control through stabilization, using tangential blowing to achieve favorable pressure gradients, are of strong interest currently.

In the application of this concept, the engine bleedoff, thrust, and structural penalties required to achieve the foregoing aerodynamic advantages are of importance to the designer. To obtain this relationship, a knowledge of the associated flowfields is required. Although attention has been given to the jet flap in theoretical investigations, relatively little analysis has been performed on upper surface blown configurations. For incompressible speeds, the work of Spence[1] represents the classical thin airfoil treatment of the jet flap problem. Other refinements of this treatment of the subsonic problem are exemplified by analyses such as those contained in Refs. 2-4. At transonic speeds, a full potential formulation with results for airfoils at zero incidence was developed by Ives and Melnik in Ref. 5. A subsequent incompressible treatment using a numerical method with certain features resembling those applied in Ref. 5 with treatment of relevant singularities was given by O'Mahoney and Smith in Ref. 6. Toward achieving a tractable three-dimensional generalization to treat blown wings as well as the incidence case, transonic small disturbance solutions were developed in Refs. 7 and 8. In these analyses, the classical Karman-Guderley model was applied with a generalized version of the Murman-Cole successive line over-relaxation scheme[9] to treat the free-jet boundaries. Both previous full potential and small disturbance models have assumed a thin or rudimentarily simple (one-dimensional) jet model. In the small disturbance formulation, it was furthermore assumed on a heuristic basis that the Spence boundary conditions were applicable across the jet. These conditions involve equilibration between the normal pressure gradient and the centrifugal force associated with the momentum in the jet. Qualitatively similar relations have been applied in full potential analyses such as those of Refs. 5 and 6.

In this paper, the applicability of the conditions will be analyzed for a compressible rotational jet in the context of blowing upstream of the trailing edge on the upper surface, i.e., upper surface blowing in contrast to the jet flap configuration in which the jet emanates from the trailing edge. For this purpose, the thin jet model will be retained, but a study of the fine structure of the jet, using asymptotic methods, will be utilized to critically evaluate the validity of the Spence conditions.

In this connection, an investigation of similar structures for the specialized problem of an oblique inviscid incompressible jet impinging on a plane, parallel flow is given in Ref. 10. There, the jet is assumed to emanate obliquely from a slot in a plane, parallel to the main flow. In the present analysis, and the backup paper of Ref. 11, the jet detail is developed for the upper surface blowing problem, which also includes the formulation of arbitrary thickness jets.

Presented as Paper 80-0270 at the AIAA 18th Aerospace Sciences Meeting, Pasadena, Calif., Jan. 14-16, 1980; submitted Feb. 22, 1980; revision received April 20, 1981.

*Manager, Fluid Dynamics. Associate Fellow AIAA.
†Mathematical Sciences Group.
‡Professor, Structures and Mechanics Department. Fellow AIAA.
§Professor, Department of Mathematics.

Furthermore, the thin airfoil jet flap problem formulation stipulates an initial angle of the jet at the trailing edge. In actuality, this angle could be a function of the jet exit conditions and the local flow details for jet flaps and USB. In both cases, the conditions for the trailing-edge dividing streamline represent a generalization of the Kutta condition for the unblown case, and is studied herein.

The aspect of the paper involving the details of the jet layer represents an extension of the earlier work of Malmuth and Murphy[12] on transonic wall jets. From these analyses, the paper will describe the numerical approach to treat the USB problem, and various results showing possibilities for lift augmentation will be presented. An additional significance of the work is its relevance to the wake curvature effects treated by Melnik and his co-workers[13] for viscous flow over transonic airfoils.

In Sec. II, various formulations and analyses are provided which represent, in part, a critical assessment of different aspects of the jet flap formulation given in Ref. 1 and its extension to USB for incompressible and compressible flows. As a basis for the thin airfoil and small disturbance models, the thin jet approximation is described in terms of a systematic asymptotic expansion procedure in Sec. II.A for incompressible flows. The generalization of these developments to compressible flow is straightforward and therefore not provided. Section II.B provides a discussion of the trailing-edge region from the viewpoint of a nonuniformity of the thin jet theory, as well as the generalized Kutta condition for USB. Inherent in this aspect is the geometry of the dividing streamline at the trailing edge, which is a necessary condition for the determination of the jet sheet free boundary. Arguments are provided to substantiate tangency to the upper surface providing the jet stagnation pressure is greater than that of the external flow. Also indicated is how the small disturbance jet flap formulation of Ref. 1 is modified with USB. Finally, Sec. III gives results from a computational solution based on the small disturbance formulation of the earlier sections. In this section, transonic USB airfoils are analyzed and comparisons are made with experiment. Factors associated with the discrepancies are considered, and refinements are proposed to improve the realism of the model.

II. Formulations and Analyses

A. Thin Jet Theory

As an essential ingredient of a small disturbance formulation, the jet structure is developed in this section for purposes of specification of the boundary conditions. In particular, it will be shown how the Spence theory of Ref. 1 can be derived from a systematic approximation procedure.

Referring to Fig. 1, a section of the jet is shown. A curvilinear coordinate system is embedded in the jet as indicated. The lines $\eta = \text{const}$ are parallel to a reference line (the ξ axis) which is the (flux) centerline if the jet is symmetric, or the wall for a wall jet case. In this coordinate system, the lines $\xi = \text{const}$ are normals to ξ axis. In what follows, the incompressible case will be discussed. The generalization to compressible flow are straightforward.

Within the indicated coordinate system, the exact equations of motion are

Continuity

$$\frac{\partial}{\partial \xi} q_\xi + \frac{\partial}{\partial \eta} h q_\eta = 0 \tag{1a}$$

ξ-momentum

$$\frac{q_\xi}{h}\frac{\partial q_\xi}{\partial \xi} + q_\eta \frac{\partial q_\xi}{\partial \eta} + \frac{q_\xi q_\eta}{h}\frac{\partial h}{\partial \eta} = \frac{-1}{\rho h}\frac{\partial p}{\partial \xi} \tag{1b}$$

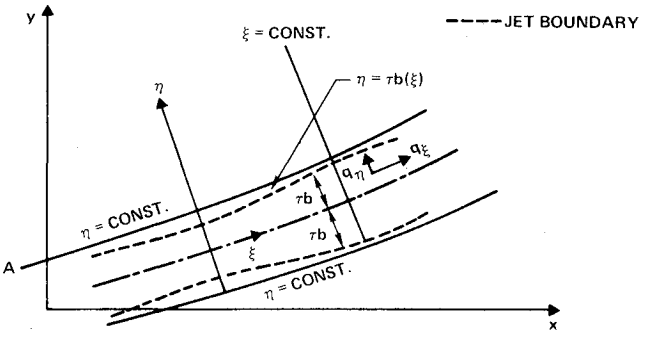

Fig. 1 Section of jet and curvilinear coordinate system.

η-momentum

$$\frac{q_\xi}{h}\frac{\partial q_\eta}{\partial \xi} + q_\eta \frac{\partial q_\eta}{\partial \eta} - \frac{q_\xi^2}{h}\frac{\partial h}{\partial \eta} = -\frac{1}{\rho}\frac{\partial p}{\partial \eta} \tag{1c}$$

where h, the metric coefficient when related to the differential arc length in Cartesian (x,y) coordinates is

$$dx^2 + dy^2 = h^2(\xi,\eta)d\xi^2 + d\eta^2, \quad h(\xi,\eta) = 1 - \eta/R(\xi) \tag{2}$$

with $R(\xi)$ being the radius of curvature which is shown positive in Fig. 1.

To obtain an approximate incompressible set of equations prototypic of the compressible case, the thin jet limit is considered. The characteristic jet thickness is shown in Fig. 1, where the jet boundary is denoted as $\eta = \tau b(\xi)$. The quantity τ thus represents a characteristic slope of the jet free boundaries which is of the same order as the jet thickness in units of its radius of curvature.

We now define a thin jet limit

$$\tau \to 0, \quad \xi, \eta^* = \eta/\tau \quad \text{fixed} \tag{3}$$

where the boundary layer coordinate η^* is introduced to keep the jet slip lines in view in the limit process. In Eq. (3), the appropriate representations to yield a nontrivial structure are

$$\frac{q_\xi(\xi,\eta;\tau)}{U} = \frac{1}{\sqrt{\tau}} u_0(\xi,\eta^*) + \sqrt{\tau} u_1(\xi,\eta^*) + \ldots \tag{4a}$$

$$q_\eta/U = \sqrt{\tau} v_0 + \tau^{3/2} v_1 + \ldots \tag{4b}$$

$$p/\rho U^2 = p_0 + \tau p_1 + \ldots \tag{4c}$$

where U is some typical freestream velocity. The orders were selected to give the "richest" possible set of equations and, consistent with this, to produce forcing terms in the equations for the second-order quantities. These orders are consistent with the massless momentum source model of Spence.[1]

Substitution of Eq. (4) in Eq. (1) and equating like orders gives the following equations for the approximate quantities:

$$\frac{\partial u_0}{\partial \xi} + \frac{\partial v_0}{\partial \eta^*} = 0 \tag{5a}$$

$$u_0 \frac{\partial u_0}{\partial \xi} + v_0 \frac{\partial u_0}{\partial \eta^*} = 0 \tag{5b}$$

$$\frac{u_0^2}{R(\xi)} = -\frac{\partial p_0}{\partial \eta^*} \tag{5c}$$

$$\frac{\partial u_1}{\partial \xi} + \frac{\partial v_1}{\partial \eta^*} = \frac{1}{R}\frac{\partial}{\partial \eta^*}(\eta^* v_0) \tag{6a}$$

$$u_0\frac{\partial u_1}{\partial \xi}+v_0\frac{\partial u_1}{\partial \eta^*}+\frac{\partial u_0}{\partial \xi}u_1+\frac{\partial u_0}{\partial \eta^*}v_1$$

$$=\frac{u_0v_0}{R}-\frac{\eta^*}{R}u_0\frac{\partial u_0}{\partial \xi}-\frac{\partial p_0}{\partial \xi} \tag{6b}$$

$$\frac{2u_0u_1}{R}+\frac{\partial p_1}{\partial \eta^*}=-u_0\frac{\partial v_0}{\partial \xi}-v_0\frac{\partial v_0}{\partial \eta^*}-\frac{u_0^2\eta^*}{R^2} \tag{6c}$$

The appropriate boundary conditions involve statements regarding the fact that the jet boundaries are streamlines and that the static pressure is continuous across the slip lines. The upper and lower slip lines S_u and $S_\ell=0$ are given by

$$S_u=\eta-\tau b_0(\xi)-\tau^2 b_1(\xi)=0$$

$$S_\ell=\eta+\tau b_0(\xi)+\tau^2 b_1(\xi)=0$$

where symmetry has been assumed to leading order.

Based on the foregoing discussion, the condition that jet boundaries S are streamlines is

$$q\cdot\nabla S=0$$

where $q=(q_\xi,q_\eta)$. Substitution of the expansions (4) into this relation gives

$$v_0(\xi,b_0)=b_0'(\xi)u_0(\xi,b_0) \tag{7a}$$

$$v_0(\xi,-b_0)=-b_0'(\xi)u_0(\xi,-b_0) \tag{7b}$$

$$v_1(\xi,b_0)=\frac{v_0(\xi,b_0)b_0}{R}+b_1b_0'\frac{\partial u_0}{\partial \eta^*}(\xi,b_0)+u_1(\xi,b_0)b_0'$$

$$-b_1\frac{\partial v_0}{\partial \eta^*}(\xi,b_0)+b_1u_0(\xi,b_0) \tag{7c}$$

$$v_1(\xi,-b_0)=-\frac{v_0(\xi,-b_0)b_0}{R}+b_1b_0'\frac{\partial u_0}{\partial \eta^*}(\xi,-b_0)$$

$$-u_1(\xi,-b_0)b_0'+b_1\frac{\partial v_0}{\partial \eta^*}(\xi,-b_0)-b_1u_0(\xi,-b_0) \tag{7d}$$

The other conditions involving continuity of pressure are

$$p_0(\xi,b_0)=\frac{p_{\text{ext}}^{(u)}(\xi)}{\rho U^2}\equiv q_u(\xi) \tag{8a}$$

$$p_1(\xi,b_0)=-b_1(\xi)\frac{\partial p_0}{\partial \eta^*}(\xi,b_0) \tag{8b}$$

where we assume for the present argument that the external pressure field $p_{\text{ext}}^{(u)}$ is prescribed. Similar pressure conditions hold for the lower slip line boundary. If δ is a characteristic flow deflection angle of the order of the airfoil thickness or angle of attack, then $\tau\ll\delta$ has also been implicitly assumed.

Solutions

First-Order Theory: We introduce the zeroth order stream function given by

$$\frac{\partial\psi}{\partial\xi}=-v_0 \qquad \frac{\partial\psi}{\partial\eta^*}=u_0$$

and employ the following transformation for the independent variables

$$(\xi,\eta^*)\rightarrow(\xi,\psi) \tag{9}$$

Under Eq. (9), the differential operators map as follows:

$$\frac{\partial}{\partial\xi}=\frac{\partial}{\partial\xi}-v_0\frac{\partial}{\partial\psi}, \qquad \frac{\partial}{\partial\eta^*}=u_0\frac{\partial}{\partial\psi}$$

and Eqs. (5) become

$$\frac{\partial u_0}{\partial\xi}-v_0\frac{\partial u_0}{\partial\psi}+u_0\frac{\partial v_0}{\partial\psi}=0 \tag{10a}$$

$$\frac{\partial u_0}{\partial\xi}=0 \tag{10b}$$

$$\frac{u_0}{R}=-\frac{\partial p}{\partial\psi} \tag{10c}$$

The general solution of Eqs. (10) is

$$u_0=u_0(\psi) \tag{11a}$$

$$p_0=k(\xi)=\frac{1}{R(\xi)}\int_0^\psi u_0(\psi')\,d\psi' \tag{11b}$$

$$v_0(\xi,\psi)=b'(\xi)u_0(\psi) \tag{11c}$$

where $k(\xi)$ is the pressure on the centerline. The reference (centerline) condition $[v_0(\xi,0)=0]$ or the conditions at the edges of the jet [Eqs. (7b)] show that $b'\equiv0$ and $b_0=1$, if $b_0(0)=1$. Thus, in terms of an arbitrary initial parallel flow profile $u_0=f(\eta^*)$ at $\xi=0$, we have

$$\psi=\int_0^{\eta^*}f(\tilde\eta)\,d\tilde\eta \tag{12a}$$

Therefore, $u_0=f(\eta^*(\psi))$, and

$$p_0(\xi,\psi)=k(\xi)-\frac{1}{R(\xi)}\int_0^\psi f(\eta^*(\psi))\,d\psi$$

$$=k(\xi)-\frac{1}{R}\int_0^{\eta^*}f^2\,d\eta^*=q_u(\xi)+\frac{1}{R}\int_{\eta^*}^1 f^2\,d\eta^* \tag{12b}$$

$$k(\xi)=q_u+\frac{1}{R}\int_{\eta^*}^1 f^2\,d\eta^* \tag{12c}$$

Discussion

Equations (12) describe a parallel flow jet. The total jump in pressure across the jet from Eq. (12c) is

$$[p_0]=p(\xi,1)=p(\xi,-1)=-\frac{2}{R}\int_0^1 f^2(\eta^*)\,d\eta^* \tag{13}$$

which agrees with the Spence model. It should be noted that, in contrast to the latter, no assumption regarding irrotationality is required to obtain Eq. (13), unlike the results of previous workers. The radius of curvature of the jet is approximately R upstream of the trailing edge, which, in turn, is given approximately by that of the blown upper surface. Downstream of the trailing edge, R is determined from applying Eq. (13) to the determination of the flow outside the jet. Upstream of the trailing edge, the wall pressure is determined by Eq. (13), since R is known and is given by

$$p(\xi,-1)=q_u(\xi)+\frac{2}{R}\int_0^1 f^2(\eta^*)\,d\eta^* \tag{14}$$

In Ref. 11, the appropriate second-order theory corresponding to the expansions (4) is derived. Also indicated are

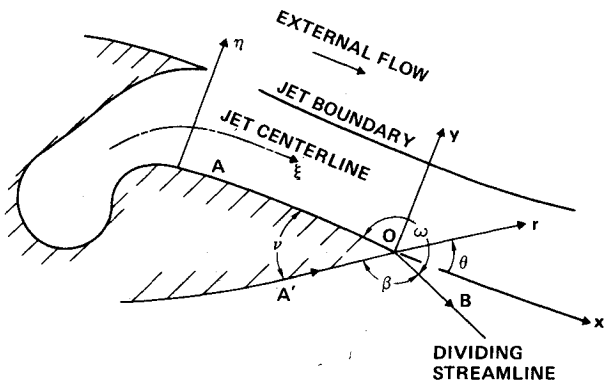

Fig. 2 Blown trailing-edge formulation.

various nonuniformities that can occur, such as those near the trailing edge. These reveal the need for other expansions in the neighborhood of the nonuniformities.

Also in Ref. 11, a small deflection specialization of the previous thin jet theory is considered. Therein, a systematic patching procedure is utilized employing a "blending layer" at a vertical distance of the order of the slip line and airfoil deflection angle δ as $\delta \to 0$. The blending layer has been used to validate the usual Taylor's series transfer of boundary conditions employed to define the outer flow. A treatment of similar blending layers is discussed in Cole[14] in connection with incompressible flows around unblown bodies of revolution.

B. Trailing-Edge Behavior

Incompressible Flows

Defining the complex potential function as

$$F(z) = \phi(x,y) + i\psi(x,y)$$

where (x,y) is the local coordinate system shown in Fig. 2 and $z = x + iy$, the local "corner flow" solution to within a dimensional multiplicative constant in the lower external region $A'OB$, with β as the dividing streamline angle shown, is given by

$$F = e^{-i\pi(\pi+\nu)/\beta} z^{\pi/\beta} \tag{15}$$

which implies that the square of the resultant velocity q is

$$|F'|^2 = q^2 \sim r^{2[(\pi/\beta)-1]} \tag{15'}$$

The initial conditions for determination of the jet follow from the requirement that the pressure and flow angle be continuous across the dividing streamline near the trailing edge were studied for incompressible flow. Referring to Fig. 2, with the dividing streamline denoted as OB, we signify the trailing-edge angle as ν, the angle that OB makes with the upper surface AO as ω and that with the lower surface as β. The details of this discussion are given in Ref. 11, which shows that $\omega = \pi$ and $\beta < \pi$ is the only viable possibility if the stagnation pressure p_0^+ above AOB is greater than that below it, which is signified by p_0^-, where + and − superscripts signify conditions above and below the slip line AOB, respectively, and 0 refers to stagnation conditions. Denoting u as the flow speed along the slip line, Bernoulli implies

$$u^+ = \sqrt{[2(p_0^+ - p_0^-)]/\rho}$$

Here also, $u^- = 0$. These results quantify the slip.

If, on the other hand, $p_0^+ < p_0^-$, then $\omega < \pi$ and $\beta = \pi$ is the only possibility with

$$u^- = \sqrt{[2(p_0^- - p_0^+)]/\rho} \qquad u^+ = 0$$

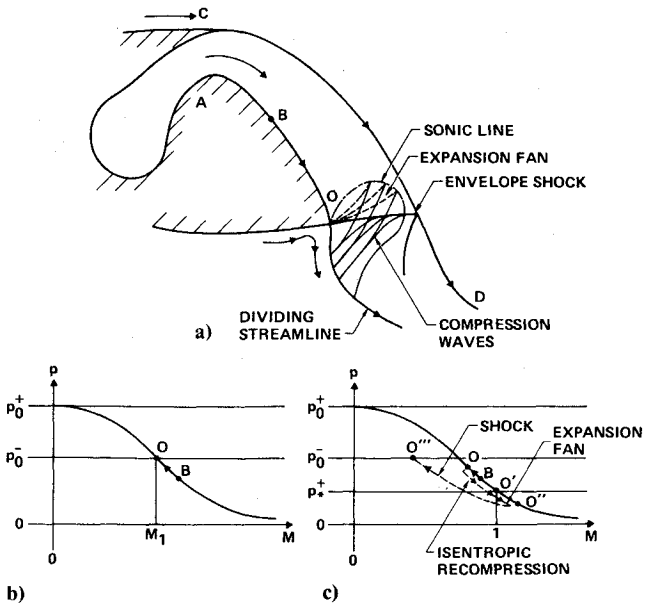

Fig. 3 a) Multivalued pressure at trailing edge—configuration for dividing streamline (discontinuous configuration); b) continuous isentropic recompression; c) discontinuous configuration.

For a hypothetical case in which $p_0^- \approx p_0^+$ in a real physical flow (fluctuating above and below equality), then a tristable configuration could evolve which would oscillate between configurations in which the dividing streamline is tangent to the upper or lower surface or bisects the trailing-edge angle. Similar arguments have been applied to treat the conditions of the stream sheet at the trailing edge of unblown incompressible three-dimensional wings in Ref. 15.

Nonuniformities of Second-Order Approximation

From Eq. (15), we find that another nonuniformity associated with second-order solutions discussed in Ref. 11 is related to the following behavior:

$$q_u' \sim r^{(2\pi/\beta)-3} \quad \text{as} \quad r \to 0$$

where, we distinguish the following possibilities as $\xi \to \xi_{TE}$:

1) $q_u' \to \infty$, $\beta > 2\pi/3$ or $\nu < \pi/3$

2) $q_u' \to 0$, $\beta < 2\pi/3$ or $\nu > \pi/3$

3) q_u' finite $\neq 0$, $\beta = 2\pi/3$ or $\nu = \pi/3$

Case 1 is the most practical situation and could necessitate an inner solution for the transition layer to join the wall and free-jet flows. This aspect is discussed in Ref. 11. For the jet structure considered here, we briefly investigate the vorticity, which can be shown to be given by

$$\omega = \tau^{-3/2}\omega_0 + \tau^{-1/2}\omega_1 + \ldots$$

where, as an illustration, if $u_0 = C$, then

$$\omega_0 = \frac{\partial u_0}{\partial \eta^*} = 0$$

$$\omega_1 = \frac{\partial u_1}{\partial \eta^*} - \frac{u_0}{R} = -\frac{C}{R(0)} = \text{const} \neq 0$$

Because of the constant initial velocity profile, a nonzero vorticity is introduced by the body curvature. By contrast, a potential vortex over a circular cylindrical surface would have had a linear initial profile to produce an irrotational flow.

Note for arbitrary initial profiles, $u_0(0,\eta^*)=f(\eta^*)$ and thus $\omega_0=f'(\eta^*)\neq 0$.

Compressible Trailing Edges

Consider again the configuration of Fig. 2. Here we analyze first the case where $p_0^+ > p_0^-$. With the usual isentropic relation

$$\frac{p^+}{p_0^+}=\left[1+\frac{\gamma-1}{2}M^2\right]^{\frac{-\gamma}{\gamma-1}} \quad (p^+ = \text{static pressure on upper side})$$

the local Mach number M can adjust in a continuous way so that the flow recompresses smoothly from B to O. At O, M is single valued ($=M_1$) and adjusts itself such that the static pressure $p^+ = p_0^-$, in accord with the isentropic relation, assuming that the flow stagnates at O on the lower side. The only way this can be realized is with the $\omega=\pi$ and $\beta<\pi$ configuration. By contrast, a discontinuous transition can occur, and is illustrated schematically in Fig. 3a, and is associated with an $\omega>\pi$ and $\beta<\pi$ arrangement. In some respects the configuration resembles flow over a solid wall expansion corner consisting of expansion fan interacting with a sonic line from the corner. If the solid configuration were representative of this flow with the free boundary slip line, compression waves would reflect off the sonic line and form a shock envelope which would be necessary to recompress the flow from an overexpanded value below the critical p_*^+ to the p_0^- level. Additional reflections can be produced from the upper slip line CD. This discontinuous transition leads to a multivalued pressure at O. The continuous and discontinuous processes are illustrated schematically in Figs. 3b and 3c, respectively. In Fig. 3b, the recompression takes place on the line BO. In Fig. 3c it occurs on $OO'O''O'''$, signifying the confluence of multiple states at O. Here, the dashed line element $O''O'''$ signifies a shock jump. Experimental data strongly suggest that as in the incompressible case, the configuration with $\omega=\pi$ and $\beta<\pi$ is the most probable situation. A more rigorous argument to support this conjecture could rely on a stability analysis. Specific criteria to determine whether the discontinuous or continuous configuration occurs in a given case is an open question that requires further study.

For $p_0^+=p_0^-$, the dividing streamline would again bisect the trailing edge, since the flow in the immediate vicinity would be incompressible and the reasoning in the previous section would apply. For the improbable case of $p_0^+<p_0^-$, the configuration with $\omega<\pi$ as $\beta=\pi$ would be applicable as for the incompressible situation.

External Flow

For distances large compared to the jet width, the fine structure of the jet is important only insofar as it provides matching conditions to the irrotational "outer" flowfield. In incompressible flow, this external outer flow can be determined by thin airfoil theory. At transonic speeds, small disturbance theory is appropriate for this region. Details of the asymptotic matching procedure have been discussed for incompressible flow in Ref. 11. Based on these developments and the earlier ones for thin jets in this paper, the boundary conditions for the outer flow in the incompressible and transonic cases for the jet flap and upper surface blowing are now indicated.

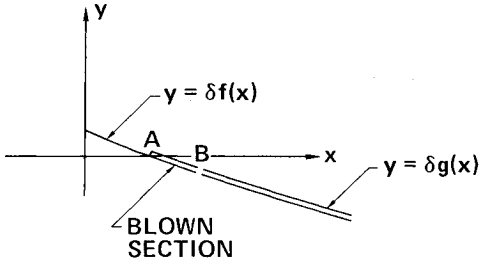

Fig. 4 Configuration for outer USB problem.

Jet Flap

Referring to Fig. 4, the equation of an airfoil can be given as $y=\delta f(x)$ and the jet is $y=\delta g(x)$ where δ is the thickness ratio of the airfoil, f is the upper or lower surface and involves the angle of attack which is assumed to be of the same order of δ. Considering a small disturbance approximation, we obtain

$$R^{-1}=\frac{d^2y/dx^2}{[1+(dy/dx)^2]^{3/2}}=\frac{\delta g''}{[1+\delta^2 g'^2]^{3/2}}\doteq\delta g''(x)$$

Letting the "outer" expansion pressure coefficient be represented as

$$(p-p_\infty)/\rho U_\infty^2=\delta P(x,y)+\ldots$$

then by virtue of a generalization of Eq. (13)

$$[P(x,0)]=-C_j g''(x)=-2[\phi_x] \tag{16}$$

where

$$C_j\equiv\rho\int_{-\tau}^{\tau} q_\xi^2 d\eta\Big/\rho U_\infty^2=0(1) \tag{17a}$$

and ϕ is a perturbation potential.

Equation (16) is the relation used in conjunction with the jet tangency relation

$$\phi_y(x,0)=g'(x) \tag{17b}$$

and the airfoil boundary conditions to determine the external flowfield. These relations coincide with the relations derived by Spence. They can be generalized for transonic flow by placing the ρ inside the integrand in Eq. (17a).

Upper Surface Blowing

To treat conditions on the blown part of the airfoil, Eq. (16) can be applied by approximating the radius R by $(f'')^{-1}$ to obtain the wall pressures, and by using the airfoil and jet boundary conditions to determine the upper slip-line jet pressures.

From the thin jet theory derived earlier, it can be seen that rotational flow produces the same pressure jumps across the jet in the dominant approximation as the irrotational Spence models. Correspondingly, it can be shown that to within factors involving the density, qualitatively similar results are obtained for transonic flow. Another important aspect of the asymptotic representations derived here is that they lead to higher approximations for the structure of the jet and external flow which can be systematically obtained. Finally, the analytical solutions described above and in Ref. 11 allow the systematic assessment of the effects of initial vorticity and skewness which are inaccessible to other theories.

III. Results and Discussion for Transonic Upper Surface Blowing

A successive line over-relaxation (SLOR) scheme within a Karman-Guderley framework has been used to compute the flowfield over an upper surface blown airfoil. On the blown portion, the jump conditions across the jet are determined by the asymptotic results given in previous sections, i.e., Eqs. (16) and (17b). Provided that the region is not too close to the jet exit or trailing edge, the streamwise gradients can be neglected in the entropy and velocity component parallel to the wall. Away from these regions, the pressure gradient perpendicular to the streamlines is balanced by centrifugal

force. For the region near the jet exit, these assumptions become invalid. Here, the scale of the gradients in the streamwise direction becomes important, principally because of the influence of wave interactions with the slip line. Similar fine structures occur near the trailing edge where the flow can stagnate on the unblown side, depending on the ratio of the stagnation value. For incompressible flow, the previous sections have discussed the tristable equilibrium at the trailing edge corresponding to the value of the stagnation pressure ratio, which leads to the dividing streamline leaving tangent to the upper surface if this is greater than unity. Consistent with the previous discussion, the appropriate generalization to transonic flow was assumed also to be this arrangement for a single-valued pressure without a shock in that location. This assumption has been altered to assess the sensitivity of the flow to the dividing streamline angle. In this connection, surface pressures for the dividing streamline bisecting the trailing-edge angle (as it would in incompressible flow) were compared with those for the tangent arrangement. Based on these studies, significant differences are anticipated only for large incidences and trailing-edge angles.

Typical results obtained from the computational model are shown in Fig. 5, in which the flow over a thick airfoil designed at Rockwell's Columbus Aircraft Division (NAAD) was analyzed with the SLOR code. Here, the pressures for various values of the blowing coefficient C_j are compared against those for the unblown case at a freestream Mach number $M_\infty = 0.703$, and angle of attack $\alpha = 0$ deg. Substantial lift augmentation is evident for blowing. Also evident is the associated rearward motion of the shock with increased blowing and sectional loading as if the incidence is increased.

Further parametric studies are provided in Fig. 6 which indicate the effect of parallel displacement of the slot (x_j in units of the chord), on the chordwise pressures. Three positions of the slot $x_j = 0.5$, 0.65, and 0.8 are shown. No systematic trend in the blown pressures is exhibited on this airfoil with downstream slot movement for fixed C_j. Evident, however, is a slight intensification of the terminating shock with slot downstream motion although its position remains unaltered. Despite the limitations of the model to describe the fine structure of the jet exit region, a small suction peak which has been observed in experiments is exhibited in this vicinity for $x_j = 0.5$. In Fig. 7, the corresponding increase in lift coefficient C_L with slot downstream movement is also shown, as well as the increase in the size of the supersonic region.

In Fig. 8, the increase of lift with blowing coefficient as well as size of the supersonic region is quantified.

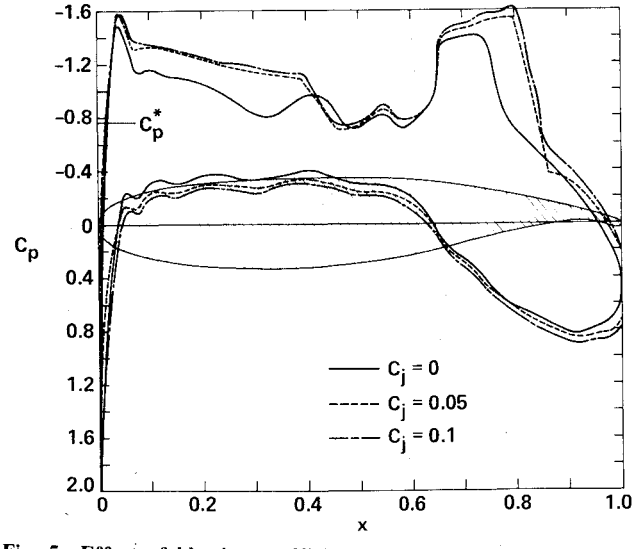

Fig. 5 Effect of blowing coefficient (C_j) variations on chordwise pressures for CAD USB supercritical airfoil, $M_\infty = 0.703$, $\alpha = 0$ deg (slot location at 65% chord).

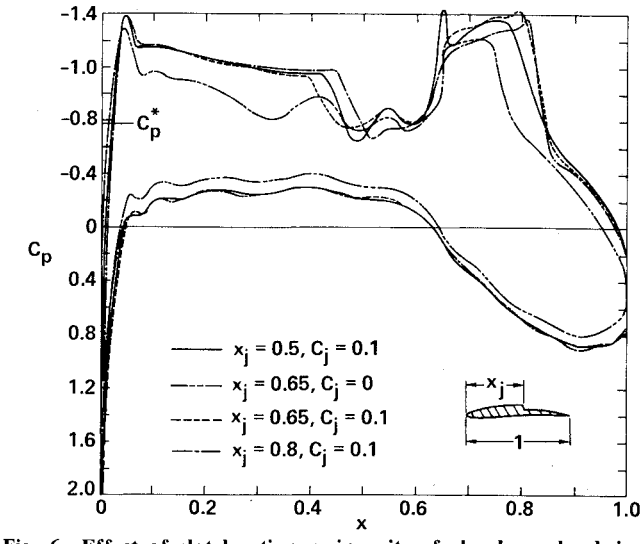

Fig. 6 Effect of slot location x_j in units of chord on chordwise pressures for CAD USB supercritical airfoil, $M_\infty = 0.703$, $\alpha = 0$ deg.

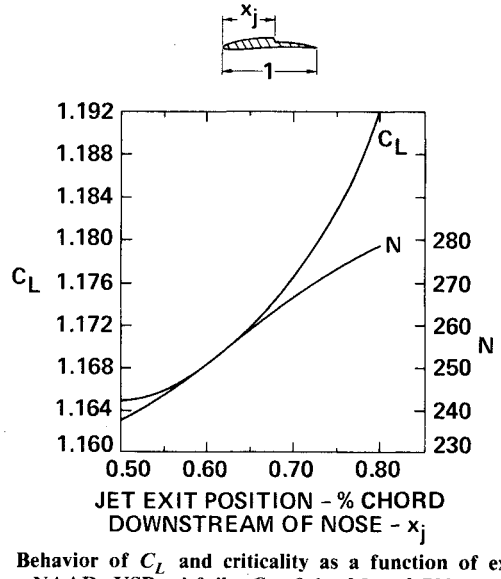

Fig. 7 Behavior of C_L and criticality as a function of extent of blowing, NAAD USB airfoil, $C_j = 0.1$, $M_\infty = 0.703$, $\alpha = 0$ deg, N = number of supersonic points.

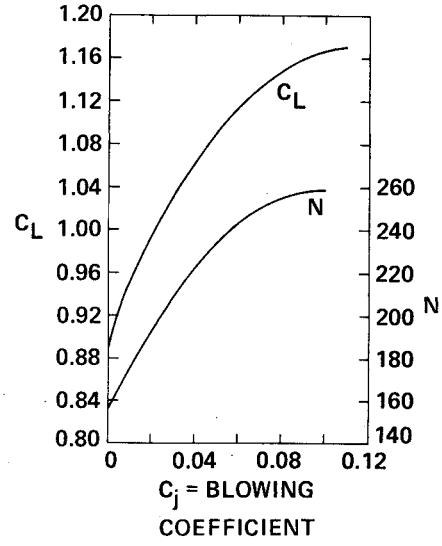

Fig. 8 Variation of C_L and criticality of CAD USB airfoil with blowing coefficient, $M_\infty = 0.703$, $\alpha = 0$ deg, $x_j = 0.65$, N = number of supersonic points.

Tests of the adequacy of the foregoing model to simulate realistic transonic USB airfoil flows have been inhibited by the lack of suitable experimental data. Information exists only for highly three-dimensional configurations, large thickness, or incidence in ranges beyond the validity of the assumptions of small disturbance theory. Another restriction is the unavailability of the associated geometric data and flow diagnostics accompanying the tests. The results of Yoshihara and his co-workers were useful in this connection and allowed us to compare the jet flap specialized version of the USB theory in Ref. 16. For the simulations described in this paper, tests performed by Freeman at NPL on a USB modified 6% thick RAE 102 airfoil, and described in Ref. 17 appear to be the most suitable results for comparison at present. Unfortunately, the angle of attack associated with the NPL data is 6 deg, which is marginal for the application of a small disturbance model.

Figure 9 indicates comparisons of chordwise pressures for various values of C_j. Also shown are Schlieren photographs indicating the associated flowfield structure. Turning to the $C_j = 0$ results (Fig. 9a), massive shock-induced separation is indicated and is apparently initiated at the downstream limb of the lambda shock on the upper surface. This is reflected in the classical erosion of the suction plateau and is responsible for the indicated disagreement between the inviscid computational results and the data. For these tests, nominal tangential blowing with a slot height of 0.07% of the chord was used. The slot location is 15% downstream of the nose. The Mach number M immediately above the slip line at the slot is approximately 1.29 for both C_j's indicated. For $C_j = 0.017$, the slot Mach number M_e has been estimated as 1.79 and for $C_j = 0.048$, $M_e \approx 2.36$.

Comparison between theory and experiment in Fig. 9b indicates reduced discrepancies on the upper surface associated with the limited separation. In Fig. 9c, the agreement is correspondingly further improved.

To achieve adequate realism, it is important to discuss factors responsible for the disagreements. One feature not captured by the USB simulation is the pressure spike at the slot location. Based on the slot size, the streamwise scale for this phenomenon is at least an order of magnitude greater than the characteristic wavelength of a Mach diamond pattern in the wall jet. These fluctuations may not be resolvable with conventional pressure tap arrangements for the thin slot employed in the tests. If a rough model of a coflowing inviscid supersonic wall jet over a flat plate is used to describe the flow near the slot, the approach to a final steady state may be damped oscillatory or monotone depending on whether the reflection coefficient R, which is given by

$$R = (\lambda - 1)/(\lambda + 1) \tag{18}$$

where

$$\lambda = M_e^2\beta/M^2\beta_e \quad \beta = \sqrt{M^2 - 1} \quad \beta_e = \sqrt{M_e^2 - 1}$$

is, respectively, positive or negative.

The relaxation length L to achieve the downstream pressure in units of the exit height is of the order of $\ell n R$, which can be approximately 5-50 in the present case depending on the accuracy of the estimate for M_e. Note in this connection that

$$R < 0 \text{ for } 1 \le M \le M_e^2/\beta_e, \text{ and } M_e \le M \le \infty$$

$$R \ge 0 \text{ for } M_e^2/\beta_e \le M \le M_e$$

For the submerged case, $R \to 1$, $(M_e \gg M)$, and the Prandtl periodic pattern is obtained, with no radiation of energy to the external flow.

These facts suggest that one factor that may be responsible for the observed spike is the internal decay process in the jet. If transonic effects and wall curvature are accounted for, the presence of "ballooning" and throats in the jet may also be contributory. We have discussed such phenomena in connection with submerged transonic wall jets in Ref. 12 and have reported analogous results for the coflowing case in Ref. 18. Selection rules in terms of M_e and M for the existence of throats in the jet near field are given in Ref. 19 which are based on an integral form of the Karman-Guderley equation. A rough sketch of the wave system that could explain the spikes in Figs. 9b and 9c is shown in Fig. 10. Yet another phenomenon that would have a similar wave pattern would be a slight upward motion of the jet due to viscous mixing or a misalignment with the surface tangent at point A.

Turning now to the discrepancy of the values shown on the rear surface (downstream of 0.5c) in Fig. 9c, we note that in spite of the obvious elimination of separation, a thick viscous wall jet is present. Downstream diffusion will affect the application of the Spence relation on the blown portion as well as the shock jump. In view of the wall jet thickness shown

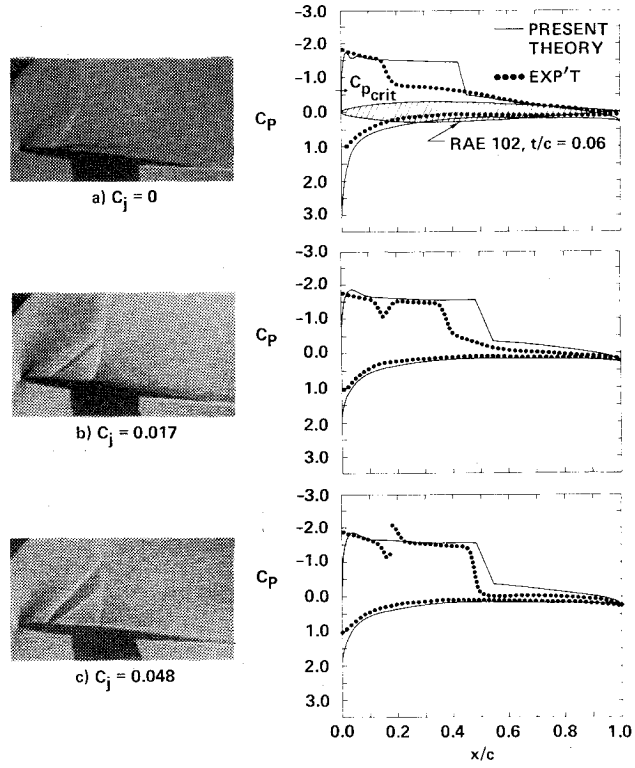

Fig. 9 Comparison of USB theory of this paper with NPL tests of Freeman,[17] $M_\infty = 0.75$, $\alpha = 6$ deg, c = chord, t = maximum thickness.

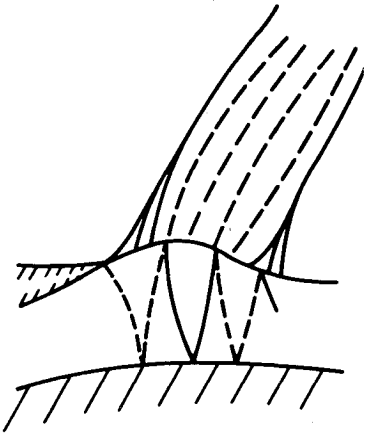

Fig. 10 Inviscid wave pattern associated with slip-line ballooning and jet throat formation.

on the Schlierens, this factor appears to be more significant than shock obliqueness at its foot. A near term refinement is being implemented, employing a coupled inviscid-viscous model using second-order boundary-layer corrections to the Spence boundary conditions accounting for axial gradients of the displacement and momentum thickness. Once these refinements are incorporated, systematic optimization among separation suppression, wave drag minimization, and supercirculation control will be possible. It is envisioned that the design techniques contained in Refs. 20-22 will augment this capability by providing methods to modulate shock formation in concert with the blowing effects.

IV. Conclusions

Asymptotic and computational models have been used to obtain the flow over upper surface blown (USB) airfoils in incompressible and transonic flow. The treatment involves a detailed analysis of the flow in the jet. The analytical and computational results indicate that:

1) In the thin jet small deflection approximation, the pressure jumps associated with the Spence theory prevail even if the flow is rotational and compressible.

2) The asymptotic developments provided herein permit further systematic refinements.

3) Effects associated with inital skewness and vorticity inaccessible to other theories can be assessed.

4) For finite trailing edge angles the dividing streamline leaves tangent to the higher stagnation pressure side if upper and lower stagnation pressures are not equal and along the trailing edge bisector if they are.

5) Computational results obtained from transonic USB configurations indicate significant enhancements of lifting pressures associated with blowing.

6) Comparisons with the experiment indicate the need for refinements incorporating wave interaction phenomena near the jet exit, as well as viscous interaction processes in the downstream portion of the wall jet.

Acknowledgment

A major portion of this effort was sponsored by the Office of Naval Research under Contract N00014-76-C-0350.

References

[1] Spence, D. A., "The Lift Coefficient of a Thin Jet Flapped Wing," *Proceedings of the Royal Society, Series A,* Vol. 238, Dec. 1956, pp. 46-48.

[2] Sato, J., "Discrete Vortex Method of Two-Dimensional Jet Flaps," *AIAA Journal,* Vol. 11, July 1973, pp. 968-973.

[3] Halsey, N. D., "Methods for the Design and Analysis of Jet Flapped Airfoils," AIAA Paper 74-188, Jan. 1974.

[4] Leoman, R. G. and Plotkin, A., "An Improved Solution of the Two-Dimensional Jet Flapped Airfoil Problem," *Journal of Aircraft,* Vol. 9, Sept. 1972, pp. 631-635.

[5] Ives, D. C. and Melnik, R. E., "Numerical Calculation of the Compressible Flow over an Airfoil with a Jet Flap," AIAA Paper 74-542, June 1974.

[6] O'Mahoney, R. and Smith, F. T., "On the Calculation of the Incompressible Flow Past an Airfoil with a Jet Flap," *Aeronautical Quarterly,* Vol. 29, Feb. 1978, pp. 44-58.

[7] Malmuth, N. D. and Murphy, W. D., "A Relaxation Solution for Transonic Flow over Jet Flapped Airfoils," *AIAA Journal,* Vol. 14, Sept. 1976, pp. 1250-1257.

[8] Murphy, W. D. and Malmuth, N. D., "A Relaxation Solution for Transonic Flow over Three-Dimensional Jet-Flapped Wings," *AIAA Journal,* Vol. 15, Jan. 1977, pp. 46-53.

[9] Murman, E. M. and Cole, J. D., "Calculation of Plane Steady Transonic Flows," *AIAA Journal,* Vol. 9, Jan. 1971, pp. 114-121.

[10] Ackerberg, R. C., "On the Nonlinear Theory of Thin Jets, Part 1," *Journal of Fluid Mechanics,* Vol. 31, Pt. 3, 1968, pp. 583-601.

[11] Malmuth, N. D., Murphy, W. D., Shankar, V., Cole, J. D., and Cumberbatch, E., "Studies of Upper Surface Blown Airfoils in Incompressible and Transonic Flow," AIAA Paper 80-0270, Jan. 1980.

[12] Malmuth, N. D. and Murphy, W. D., "An Inviscid Model for Submerged Transonic Wall Jets," AIAA Paper 77-174, 1977.

[13] Melnik, R. E., Chow, R., and Mead, H. R., "Theory of Viscous Transonic Flow over Airfoils at High Reynolds Number," AIAA Paper 77-680, June 1977.

[14] Cole, J. D., *Perturbation Methods in Applied Mathematics,* Ginn and Blaisdell, Waltham, Mass., 1968.

[15] Mangler, K. W. and Smith, J. H. B., "Behavior of the Vortex Sheet at the Trailing Edge of a Lifting Wing," *Aeronautical Journal,* Vol. 74, Nov. 1970, pp. 906-908.

[16] Yoshihara, H., Carter, W. V., Fatta, J. G., and Magnus, R. G., "Aeronautical Exploratory Research on Jet Flapped Airfoils," Convair Rept. L-112173, Feb. 1972.

[17] Pearcey, H. H., "Shock Induced Separation and Its Prevention by Design and Boundary Layer Control," *Boundary Layer and Flow Control,* edited by G. V. Lachmann, Pergamon, Oxford, London, 1961, pp. 1166-1344.

[18] Malmuth, N. and Murphy, W. D., Quarterly Letter Progress Report No. 14 on ONR Contract N00014-76-C-0350, SC5055.14QR, Aug. 20, 1979.

[19] Malmuth, N. and Murphy, W. D., Quarterly Letter Progress Rept. No. 13 on ONR Contract N00014-76-C-0350, SC5055. BQR, May 14, 1979.

[20] Shankar, V., Malmuth, N. D., and Cole, J. D., "Computational Transonic Airfoil Design in Free Air and a Wind Tunnel," AIAA Paper 78-103, Jan. 1978.

[21] Shankar, V., Malmuth, N. D., and Cole, J. D., "A Consistent Design Procedure for Supercritical Airfoils in Free Air and a Wind Tunnel," invited paper presented at NASA Langley Conference on Advanced Technology Airfoil Research, also in Proceedings, March 1978.

[22] Shankar, V., Malmuth, N. D., and Cole, J. D., "A Computational Inverse Procedure for Three-Dimensional Wings and Wing-Body Combinations," AIAA Paper 79-0344, Jan. 1979.